Original Article | Journal of Biosystems Engineering

J. of Biosystems Eng. 38(2):138-148. (2013. 6)
http://dx.doi.org/10.5307/JBE.2013.38.2.138

eISSN : 2234-1862
pISSN : 1738-1266

Kinematic and Dynamic Analyses of Human Arm Motion

Junghee Kim[1], Sungho Cho[1], Choongho Lee[2], Jaewoong Han[3], Heon Hwang[1]*

[1]*Department of Bio-Mechatronic Engineering, College of Biotechnology & Bioengineering, Sungkyunkwan University, 300 Chunchun, Jangan, Suwon, Gyeonggi, 440-746, Korea*
[2]*Department of Manufacturing and Design Engineering, College of Engineering, Jeoniu University, 300 Chunjamro, Wansan, Jeonju, Jeonbuk, 560-759, Korea*
[3]*Division of Bio-Industry Engineering, Koungju National University, Yesan 340-702, Korea*

Received: March 1st, 2013; Revised: May 24th, 2013; Accepted: May 31th, 2013

Abstract

Purpose: Determining an appropriate path is a top priority in order for a robot to maneuver in a dynamically efficient way especially in a pick-and-place task. In a non-standardized work environment, current robot arm executes its motion based on the kinematic displacements of joint variables, though resulting motion is not dynamically optimal. In this research we suggest analyzing and applying motion patterns of the human arm as an alternative to perform near optimum motion trajectory for arbitrary pick-and-place tasks. **Methods:** Since the motion of a human arm is very complicated and diverse, it was simplified into two links: one from the shoulder to the elbow, and the other from the elbow to the hand. Motion patterns were then divided into horizontal and vertical components and further analyzed using kinematic and dynamic methods. The kinematic analysis was performed based on the D-H parameters and the dynamic analysis was carried out to calculate various parameters such as velocity, acceleration, torque, and energy using the Newton-Euler equation of motion and Lagrange's equation. In an attempt to assess the efficacy of the analyzed human motion pattern it was compared to the virtual motion pattern created by the joint interpolation method. **Results:** To demonstrate the efficacy of the human arm motion mechanical and dynamical analyses were performed, followed by the comparison with the virtual robot motion path that was created by the joint interpolation method. Consequently, the human arm was observed to be in motion while the elbow was bent. In return this contributed to the increase of the manipulability and decrease of gravity and torque being exerted on the elbow. In addition, the energy required for the motion decreased. Such phenomenon was more apparent under vertical motion than horizontal motion patterns, and in shorter paths than in longer ones. Thus, one can minimize the abrasion of joints by lowering the stress applied to the bones, muscles, and joints. From the perspectives of energy and durability, the robot arm will be able to utilize its motor most effectively by adopting the motion pattern of human arm. **Conclusions:** By applying the motion pattern of human arm to the robot arm motion, increase in efficiency and durability is expected, which will eventually produce robots capable of moving in an energy-efficient manner.

Keywords: Human arm, Joint interpolation, Kinematic remodeling, Motion pattern, Manipulability, Pick-and-place task

Introduction

In general, tasks for a robot to perform are classified into two patterns, one is pick-and-place task and another is continuous path following task. A pick-and-place task has information only on the initial and final configurations of either robot arm or robot end-effector without intermediate kinematic configurations. A continuous path following task has kinematic information on intermediate configurations of robot end-effector.

In a pick-and-place task, determining the appropriate path is critical for an efficient robot maneuver. Most industrial robots, however, performs pick-and-place tasks only based on the difference of the initial and the final kinematic arm configurations. Sometimes pick-and-

***Corresponding author:** Heon Hwang
Tel: +82-31-290-7825; **Fax:** +82-31-290-7830
E-mail: bionuke@hanmail.net

place task cannot be achieved without considering a dynamic effect of robot arm maneuver. The pick-and-place motion only based on the kinematic strategy limits utilizing the full capability of a given robot arm. However, for robots that must carry out pick-and-place tasks in a non-standardized environment, it is very difficult to deal with all the situations in a dynamically optimal way. Consequently, unnecessary burden may be imposed upon the robot or the robot could bring about unintended results.

In this research we suggest applying the motion pattern of the human arm to robots as an answer to handling various unpredictable pick-and-place task situations. Humans have become capable of coping with most of predicted or unpredicted handling situations through evolution and learning. Especially in the tasks of pick-and-place whose arm trajectories were not specified exclusively, developing a human like near optimum arm motion would be the best alternative to the robot arm motion in the viewpoints of the total energy consumption, the required maximum joint torques, the minimum time to achieve the task, and so on.

As humanoids that imitate human appearance and behavior were put on spotlight in industrial manipulators, demands for robots and the associated technology have changed accordingly. Potkoniak et al. (2001) imitated and applied human motion to accomplish the task of writing with a robot arm. Pallard et al. (2002) attempted to embody natural motion of the entertainment-purpose humanoid by employing an optical motion capturing system to capture the actor's movement, but was faced with limited number of motion of the robot. Asfour and Dillmann (2000) utilized inverse kinematics in order to attain the joint variable of their humanoid ARMAR and showed the importance of considering the speed of the robot's movement.

Before applying human motion patterns to a robot, the human motion pattern must be analyzed first. Although the arm and shoulder are among the most complicated joints of our body, the following conditions by Maurel et al. (1996) may be referred for the sake of simplicity in the modeling process. The hand is an extension of the forearm as a rigid body and segments of the arm can be viewed as rigid cylinders. All joints can be assumed to be ideal kinematic joints and the muscle can be modeled only based on anatomical standard. In addition, Kodek and Munih (2003) proposed considering both static and dynamic factors when analyzing contraction and relaxation of the elbow. Mathematical methods can be applied for robot manipulator analysis to obtain the aforementioned factors (Siciliano and Sciavicco, 1998). Yoshikawa (1985) suggested the manipulability in order to quantify the manipulating ability of the end-effector. Manipulability is a measure of the variability of a posture that uses Jacobian matrix.

In Korea there have been many attempts to apply the human arm motion to robots. Jeong (2003) captured human motion and employed it to humanoids, Choi (2006) and Choi (2007) utilized stereo camera and video camera capture methods, respectively, and Lee (2007) applied optical motion capturing method to attain and analyze motion patterns. All these efforts suggested the possibility of applying human motion patterns to robots. Moreover, Bae et al. (2007) designed a robot arm with mechanical principles by focusing on the human nervous system and morphology, and demonstrated its feasibility.

In this paper vertical and horizontal motions of the human arm were analyzed by applying the principles of mechanics and dynamics in order to assess the viability of applying the human arm motion to the robot arm maneuver.

Materials and Methods

A healthy male subject (height: 181cm, weight: 88kgf) in his 20s with an intact musculoskeletal system was recruited for acquisition and analysis of the motion of the right arm. As seen in Figure 1 positions of vertical and horizontal motion were divided into eight points, spaced by 45 and 30 degrees, respectively using the motion capture system. Each vertical and horizontal motion

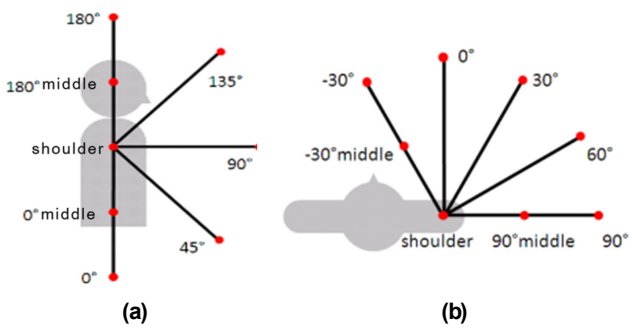

Figure 1. Position of eight primary points of (a) vertical and (b) horizontal test paths.

Table 1. Start and end positions of vertical test paths

Number	Start	End	Number	Start	End
Path 1	0°	0° middle	Path 29	90°	135°
Path 2	0° middle	0°	Path 30	0° middle	45°
Path 3	0°	45°	Path 31	45°	180°
Path 4	45°	0°	Path 32	0°	45°
Path 5	0°	90°	Path 33	45°	180° middle
Path 6	90°	0°	Path 34	180° middle	45°
Path 7	0°	135°	Path 35	45°	shoulder
Path 8	135°	0°	Path 36	shoulder	45°
Path 9	0°	180°	Path 37	90°	180°
Path 10	180°	0°	Path 38	180°	90°
Path 11	0°	180° middle	Path 39	90°	180° middle
Path 12	180°	0°	Path 40	180° middle	90°
Path 13	0°	shoulder	Path 41	90°	shoulder
Path 14	shoulder	0°	Path 42	shoulder	90°
Path 15	0°	45°	Path 43	135°	1800°
Path 16	45°	0° middle	Path 44	180°	135°
Path 17	0° middle	90°	Path 45	135°	180° middle
Path 18	90°	0° middle	Path 46	180° middle	135°
Path 19	0° middle	135°	Path 47	135°	180° middle
Path 20	135°	0° middle	Path 48	180°	shoulder
Path 21	0° middle	180°	Path 49	180°	180° middle
Path 22	180°	0° middle	Path 50	180° middle	180°
Path 23	0° middle	180°	Path 51	180°	shoulder
Path 24	180°	0° middle	Path 52	Shoulder	180°
Path 25	0° middle	shoulder	Path 53	Shoulder	180° middle
Path 26	shoulder	0° middle	Path 54	Shoulder	135°
Path 27	45°	90°	Path 55	Shoulder	180°
Path 28	90°	45°	Path 56	Shoulder	180° middle

paths generated 56 motion patterns, which yielded a total of 112 motion patterns. In order to prevent acclimation of motion and change in trace or speed due to fatigue, the order of the motion paths were randomized so that the same pattern would not be repeated consecutively. In addition the subject was given sufficient amount of rest every 10 trials.

Manipulability, Newton-Euler equation, and Lagrange's equation were used to analyze the motion patterns. The results were then compared to the joint interpolation method, a frequently used method to obtain the motion path of the robot, in order to gauge the utility of the human arm motion. Tables 1 and 2 show the start and end positions of the vertical and horizontal test paths, respectively.

In order to obtain accurate motion paths a 6-camera (MCam2) VICON 460 optical motion capturing system (Vicon Motion Systems, United Kingdom) was used to collect three dimensional coordinates from the shoulder, elbow, and wrist at a 120Hz frame rate (Figure 2). The motion capturing system operates by tracking the infrared light reflectors attached on the skin, which can introduce errors due to the movement of the skin. Thus in this research we were able to reduce errors by calibrating the shoulder as the point of origin. In addition since the speed of arm movement is relatively slow, we were able to reduce unnecessary data acquisition time by extracting 12 frames per second from the extensive data captured with a frame rate of 120Hz.

In this research we aimed to characterize the robot arm

Table 2. Start and end positions of horizontal test paths

Number	Start	End	Number	Start	End
Path 1	-30°	-30° middle	Path 29	60°	-30° middle
Path 2	-30°	0°	Path 30	60°	-30°
Path 3	-30°	30°	Path 31	60°	0°
Path 4	-30°	60°	Path 32	60°	30°
Path 5	-30°	90°	Path 33	60°	60°
Path 6	-30°	90° middle	Path 34	60°	90°
Path 7	-30°	Shoulder	Path 35	60°	Shoulder
Path 8	-30° middle	-30°	Path 36	90°	-30° middle
Path 9	-30° middle	0°	Path 37	90°	-30°
Path 10	-30° middle	30°	Path 38	90°	0°
Path 11	-30° middle	60°	Path 39	90°	30°
Path 12	-30° middle	90°	Path 40	90°	60°
Path 13	-30° middle	90° middle	Path 41	90°	90° middle
Path 14	-30° middle	Shoulder	Path 42	90°	Shoulder
Path 15	0°	-30° middle	Path 43	90° middle	-30° middle
Path 16	0°	-30°	Path 44	90° middle	-30°
Path 17	0°	30°	Path 45	90° middle	0°
Path 18	0°	60°	Path 46	90° middle	30°
Path 19	0°	90°	Path 47	90° middle	60°
Path 20	0°	90° middle	Path 48	90° middle	90°
Path 21	0°	Shoulder	Path 49	90° middle	Shoulder
Path 22	30°	-30° middle	Path 50	Shoulder	-30° middle
Path 23	30°	-30°	Path 51	Shoulder	-30°
Path 24	30°	0°	Path 52	Shoulder	0°
Path 25	30°	60°	Path 53	Shoulder	30°
Path 26	30°	90°	Path 54	Shoulder	60°
Path 27	30°	90° middle	Path 55	Shoulder	90°
Path 28	30°	Shoulder	Path 56	Shoulder	90° middle

(a) Vicon 460 (b) MCam2 (C) Position of marker

Figure 2. Optical motion capture system.

that has the human arm's shape, form, and weight when it is taking the human and robot motions through analysis based on mechanics and dynamics. All the equations in the following steps are cited from the formal robot kinematics and dynamics.

Joint interpolation method

In order to acquire the motion path of the robot arm simulating the human arm motion path, the joint interpolation method was utilized in this research. Joint interpolation method is a commonly used method to obtain the motion path of the robot and is calculated by uniformly moving the displacement from the starting point to the end point by using the robot arm's posture as shown in equation (1).

$$q_{t+1} = q_t + \frac{q_n - q_0}{n} \quad (1)$$

Here q_t is the joint variable at time t, where $0 < t \leq n$.

Kinematic remodeling

Figure 3 shows a model structure of the right arm that consists of the shoulder, elbow, and hand for mechanical analysis and Table 1 depicts Figure 3 according to the D-H parameters such as joint variable θ_i, link length a_i , link offset d_i, and twist angle α_i at the joint i.

Equation (2) shows the determination of the end-effector's position and posture by using the joint variable in forward kinematics, which can be represented as unit vector coordinate transformation matrix ${}^{i}_{}A_{i+1}$ that transforms the (i+1)th joint coordinate frame to the ith joint coordinate frame.

$$
\begin{aligned}
{}^{i}_{}A_{i+1} &= \mathrm{rot}(z_i,\theta_i)\,trans(0,0,d_i)\,trans(a_i,0,0)\,rot(x_i,\alpha_i) \\
&= \begin{bmatrix} c\theta_i & s\theta_i & 0 & 0 \\ s\theta_i & c\theta_i & 0 & 0 \\ 0 & 0 & 1 & 0 \\ 0 & 0 & 0 & 1 \end{bmatrix}
\begin{bmatrix} 1 & 0 & 0 & 0 \\ 0 & 1 & 0 & 0 \\ 0 & 0 & 1 & d_i \\ 0 & 0 & 0 & 1 \end{bmatrix} \\
&\quad \begin{bmatrix} 1 & 0 & 0 & \alpha_i \\ 0 & 1 & 0 & 0 \\ 0 & 0 & 1 & 0 \\ 0 & 0 & 0 & 1 \end{bmatrix}
\begin{bmatrix} 1 & 0 & 0 & 0 \\ 0 & c\alpha_i & -s\alpha_i & 0 \\ 0 & s\alpha_i & c\alpha_i & 0 \\ 0 & 0 & 0 & 1 \end{bmatrix} \\
&= \begin{bmatrix} c\theta_i & -c\alpha_i s\theta_i & s\alpha_i s\theta_i & \alpha_i c\theta_i \\ s\theta_i & c\alpha_i c\theta_i & -s\alpha_i c\theta_i & \alpha_i s\theta_i \\ 0 & s\alpha_i & c\alpha_i & d_i \\ 0 & 0 & 0 & 1 \end{bmatrix}
\end{aligned} \tag{2}
$$

Where, rot(z_i, θ_i) and trans(a, b, c) represent rotating θ_i around the z-axis of the ith coordinate frame and translating a, b, and c along x-axis, y-axis, and z-axis of the ith coordinate frame respectively.

In equation (2) $c\theta_i$ and $s\theta_i$ represent $\cos\theta_i$ and $\sin\theta_i$ respectively. With table 1 and equation (2) a coordinate transformation matrix with respect to the base or reference frame "0" can be constructed.

$$
{}^{0}_{}A_E = {}^{0}_{}A_1\,{}^{1}_{}A_2(\theta_1)\,{}^{2}_{}A_3(\theta_2)\,{}^{3}_{}A_4(\theta_3)\,{}^{4}_{}A_E(\theta_4)
$$

$$
\begin{aligned}
{}^{0}_{}A_E &= \begin{bmatrix} c\theta_1 & 0 & s\theta_1 & 0 \\ s\theta_1 & 0 & -c\theta_1 & 0 \\ 0 & 1 & 0 & 0 \\ 0 & 0 & 0 & 1 \end{bmatrix}
\begin{bmatrix} -s\theta_2 & 0 & c\theta_2 & 0 \\ c\theta_2 & 0 & s\theta_2 & 0 \\ 0 & 1 & 0 & 0 \\ 0 & 0 & 0 & 1 \end{bmatrix} \\
&\quad \begin{bmatrix} -s\theta_3 & 0 & c\theta_3 & 0 \\ c\theta_3 & 0 & s\theta_3 & 0 \\ 0 & 1 & 0 & 0 \\ 0 & 0 & 0 & 1 \end{bmatrix}
\begin{bmatrix} -s\theta_4 & c\theta_4 & 0 & l_4 c\theta_4 \\ c\theta_4 & s\theta_4 & 0 & l_4 s\theta_4 \\ 0 & 0 & 1 & 0 \\ 0 & 0 & 0 & 1 \end{bmatrix}
\end{aligned}
$$

where, ${}^{0}_{}A_1$ can be an identity matrix I or a fixed coordinate transformation matrix between the coordinate frame "0" and frame "1". In this case, ${}^{0}_{}A_1$ = I was used.

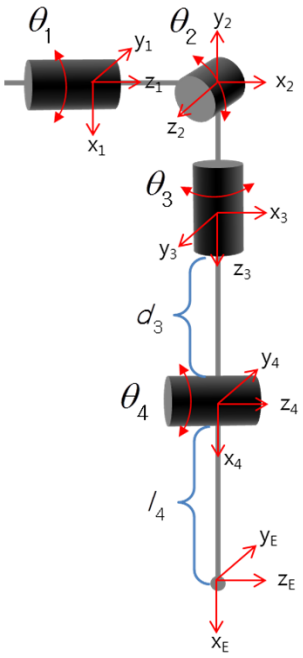

Figure 3. Structure of a human right arm.

Table 3. D-H parameters of a human arm

joint	θ_i (degree)	d_i (m)	a_i (m)	α_i (degree)
1	θ_1	0	0	90°
2	θ_2 + 90°	0	0	90°
3	θ_3 + 90°	d_3	0	90°
4	θ_4 + 90°	0	l_4	0

$$
{}^{0}_{}A_E = {}^{0}_{}A_1\,{}^{1}_{}A_2(\theta_1)\,{}^{2}_{}A_3(\theta_2)\,{}^{3}_{}A_4(\theta_3)\,{}^{4}_{}A_E(\theta_4)
= \begin{bmatrix} n_x & s_x & a_x & P_x \\ n_y & s_y & a_y & P_y \\ n_z & s_z & a_z & P_z \\ 0 & 0 & 0 & 1 \end{bmatrix} \tag{3}
$$

Where, $\begin{bmatrix} n_x & s_x & a_x \\ n_y & s_y & a_y \\ n_z & s_z & a_z \end{bmatrix}$ and $\begin{bmatrix} P_x \\ P_y \\ P_z \end{bmatrix}$ represent the orientation of the end-effector coordinate frame "E" and the position of the origin of an end-effector coordinate frame with respect to the reference coordinate frame respectively. And the first column vector denotes the normal vector of an end-effector which is x-axis of the end-effector coordinate frame "E". The second column vector denotes the sliding vector of an end-effector which is y-axis of the end-effector coordinate frame "E". The third

column vector denotes the approach vector of an end-effector which is z-axis of the end-effector coordinate frame "E". By solving 12 non-linear equations the joint variables can be obtained.

Dynamic analysis

Dynamic analysis is numerically quantifying the torque from the actuator when the arm is in motion by tracking the change in arm motion with respect to time. Typical dynamic analysis methods include the Newton-Euler equation of motion and the Lagrange's equation. Newton-Euler equation is based on Newton's second law of motion and utilizes force and moment and Lagrange's equation is based on Lagrange's function and involves work and energy. The joint torque τ_i that is being exerted on the ith joint is calculated by projecting the force and moment of each link onto the ith joint axis. In this research Newton-Euler equation of motion was used (Asada and Slotine, 1986).

Equation (4) is the coupling force and coupling moment of link i.

$$\begin{aligned} & f_{i-1,i} - f_{i,i+1} + m_i g - m_i \dot{v}_{ci} = 0 \\ & N_{i-1,i} - N_{i,i+1} + (-r_{i,ci}) \times (f_{i-1,i}) - r_{i+1,ci} \times \\ & (-f_{i,i+1}) - I_i \dot{w}_i - w_i \times (I_i w_i) = 0 \end{aligned} \quad (4)$$

$f_{i-1,i}$ = force exerted on link i by link (i-1)
$n_{i-1,i}$ = torque exerted on link i by link (i-1)
I_i = inertia tensor
w_i= angular velocity of the ith link with respect to the reference frame
$\dot{v}_{ci}$ = linear acceleration of the centroid of the ith link with respect to the reference frame
$\dot{w}_i$ = angular acceleration of the ith link with respect to the reference frame
g = gravity acceleration
$r_{i,ci}$ = distance from the origin of the ith coordinate frame to the centroid of the ith link
$r_{i,i+1}$ = distance from the origin of the ith joint coordinate frame to the origin of the (i+1)th joint coordinate frame

Where, $-m_i \dot{v}_{ci}$ is the inertial force and depicts the linear momentum change. And $-I_i \dot{w}_i - w_i \times (I_i w_i)$ is the inertial torque and depicts the angular momentum change.

By sequentially calculating the above procedure from the end-effector link to the base link, the force and moment of the respective link can be computed. As the torque of each joint represents the load being applied to the joint, the amount of torque can vary depending on the movement even within the same arm.

In order to determine the factors controlling the amount of torque, we applied Lagrange's equation (5) (Asada and Slotine, 1986).

$$\tau_i = \sum_{j=1}^{n} H_{ij} \ddot{\theta}_j + \sum_{j=1}^{n} \sum_{h=1}^{n} h_{ijh} \dot{\theta}_j \dot{\theta}_h + G_i \quad (5)$$

Where, H_{ij}, h_{ijh}, and G_i are functions of joint variables θ_1, θ_2,$\cdots$, θ_n. In equation (5) the first term represents the inertia effect, the second term represents the Coriolis and centrifugal effect, and the last term shows the effect of gravity

Manipulability

Manipulability is a quantitative criterion of the maneuverability of the robot arm that was proposed by Yoshikawa in 1983 in order to control the position and posture of the end-effector. Joint variables of n degree of freedom robot is $\theta = [\theta_1, \theta_2, \theta_3, \cdots \theta_n]^T$ and the condition vector of the end-effector is $r = [r_1, r_2, r_3, \cdots r_n]^T$, where r is depicted according to the base coordinate system of the robot system. Here m represents the number of dimensions. The geometrical relation of θ and r is given as the function in equation (6).

$$r = f(\theta) \quad (6)$$

After differentiating it with respect to time equation (7) is obtained.

$$\dot{r} = J(\theta)\dot{\theta} \quad (7)$$

Where $J(\theta)=df(\theta)/d\theta$ is the Jacobian matrix. Using the Jacobian matrix the manipulability measure W is specified as shown in equation (8) (Yoshikawa, 1983).

$$W = \sqrt{\det \boldsymbol{J}(\theta)\boldsymbol{J}^{\boldsymbol{T}}(\theta)} \quad (8)$$

Results and Discussion

In this research we assessed the suitability of applying human arm motion pattern to that of a robot arm by applying principles of mechanics and dynamics, and aimed

to prove its efficacy through comparison with motion path obtained by the joint interpolation method.

Fifty six different motion paths each for horizontal and vertical directions were configured and the human motion data for each motion path was recorded with an optical motion capture system. The acquired data had to be corrected with the joint interpolation method because of errors of joint position and length of the link introduced by the movement of the marker attached to the subjects' skin as shown in Figure 4. In addition the shoulder, which is the origin of the base link, was placed so that it would match the point of origin of the coordinates to make the analysis simpler.

To compare the motion pattern of a human arm and that of an existing robot arm, a virtual robot motion path was obtained using the joint interpolation method. Figure 6 shows an example of the human and robot motion patterns for given motion paths as shown in Figure 5. For vertical motion the farther the raised arm, the closer the hand was to the shoulder. For horizontal motion the starting and end points tended to move in a straight line.

Figure 6(a) and (b) show the vertical motion path of the human arm and corresponding virtual motion path of the robot arm created by the joint interpolation method. The difference of the kinematic movement of an end-effector and hand of human can be seen. In Figure 6(a) there is little difference between robot and human motions. Since the moment effect exerted on the shoulder joint from the gravity of an elbow and hand was not great and the initial and final configuration of arm does not need much of arm configuration change, human motion behaved similar to the robot arm motion. It showed similar pattern of movement. However, if human carries the heavy object like a 20kgf barbell and has to move the same path, the elbow should be bent and hand will move up while minimizing the length of the moment arm and then elbow will be stretched to reach the final target.

Human motion tends to move to minimize torque exer-

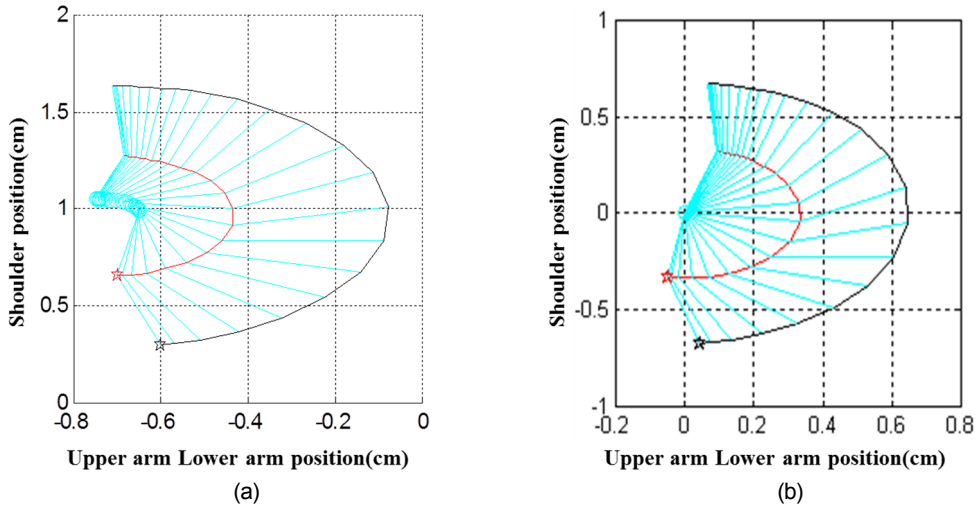

Figure 4. Trajectories (a) before and (b) after correction of the positions of origins.

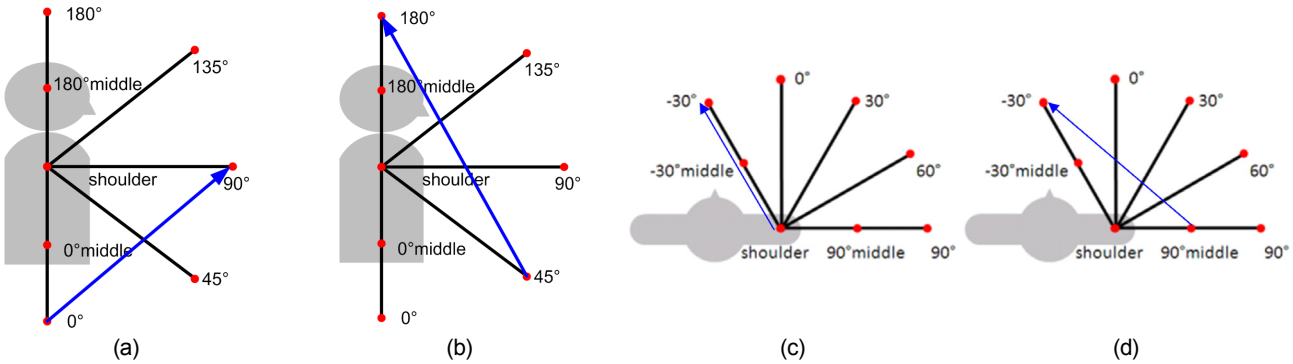

Figure 5. Example paths for the motion analysis (a): Path 19, (b):Path 31 and horizontal paths (c): Path 51, (d): Path 44.

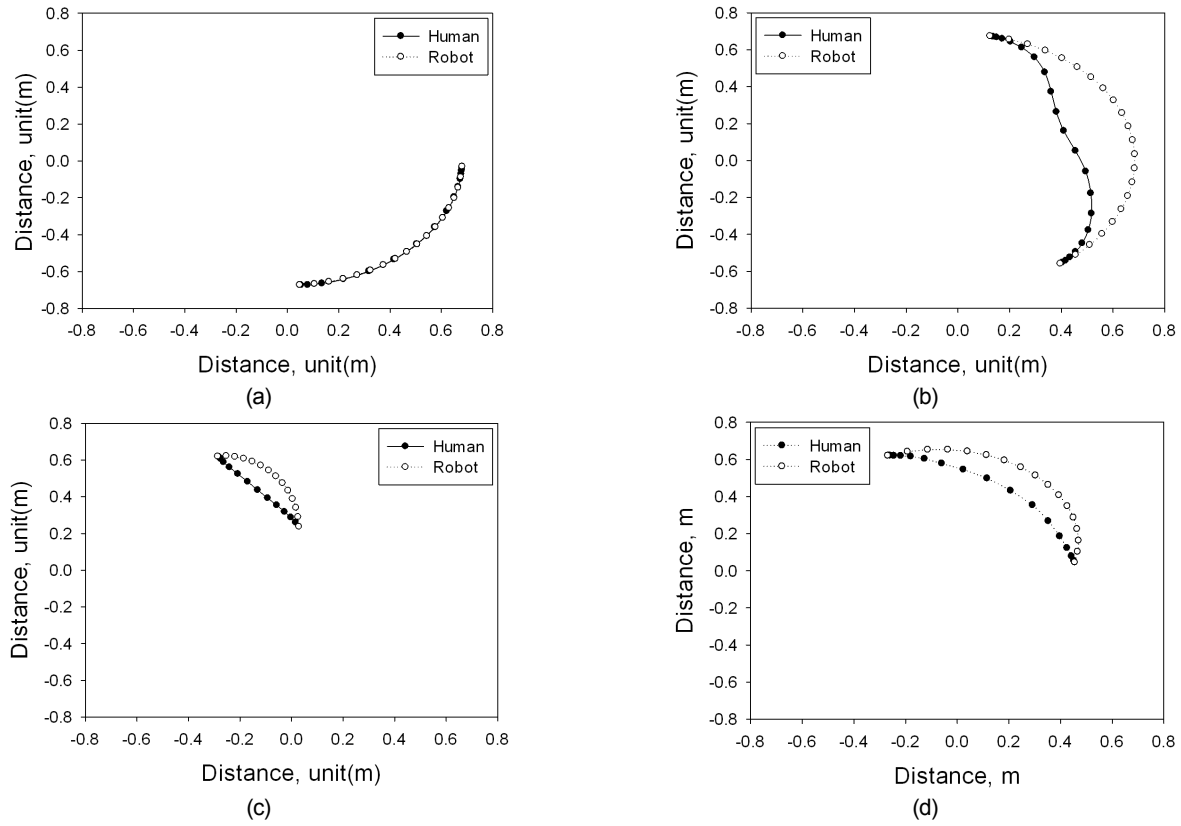

Figure 6. Examples of human and robot motion patterns of vertical paths (a): Path 19, (b):Path 31 and horizontal paths (c): Path 51, (d): Path 44.

ted on the joint especially on the shoulder joint. Bending elbow decreases the distance of the moment arm of the other link such as elbow or hand. The attribute of minimizing the amount of the exerted joint torque caused by the robot arm configuration is more intensified during the vertical motion when arm motion is executed against the gravity effect. During the horizontal motion, human tended to keep the distance of the moment arm as minimum to reduce the joint torque caused by the gravity.

Figure 7 shows the joint torque obtained by applying the Newton-Euler equation of motion to Figure 6 where torque 1 and 2 represent torque being exerted on the shoulder and the elbow, respectively. It can be seen that the human motion pattern resulted in less torque for vertical motion. This signifies the human motion pattern results in lower burden on each joint. Although it appears torque is greater in human motion for horizontal motion, but the difference between the absolute values are not significant.

What could be the reason behind the distinct difference in torque for horizontal motion? After considering various kinetic and dynamic factors we were able to find the answer to this question from effect of gravity. Figure 8 shows the gravity effect under each condition. Torque of robot motion pattern of vertical path that showed the largest difference in torque, as seen in Figure 8(b), also showed the largest difference in gravity. Human arm motion moved to reduce the torque exerted on the first shoulder joint by bending elbow. Bending elbow decreases distance of the moment caused by the gravity effect of elbow and hand.

Another answer lied in manipulability measure. Figure 9 shows the manipulability of each case. It can be observed that the greater the distance the greater the manipulability in vertical motion, but this relationship is unclear in horizontal motion when arm is relatively free of load. In addition initial and final arm configurations also affect the path of human arm. For a situation such as one joint does not need to move in order to reach the target if the torque exerted on the moving joint especially a lower joint like shoulder is relatively small, upper joint such as elbow will not be moved during the motion.

Manipulability is defined as a measure of the end-effector's ability to manipulate and is a quantitative notion

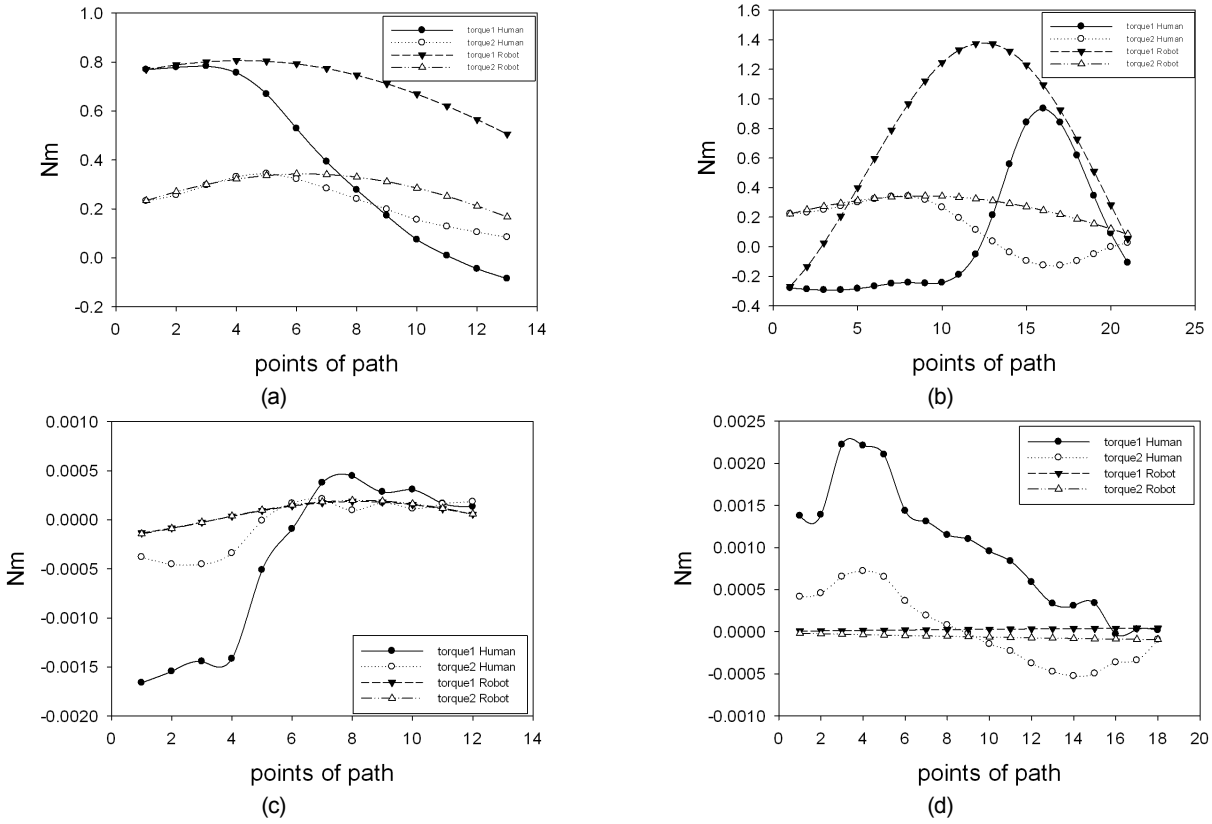

Figure 7. Torque of human and robot motion patterns of vertical paths (a): Path 3, (b):Path 27 and horizontal paths (c): Path 13, (d): Path 30.

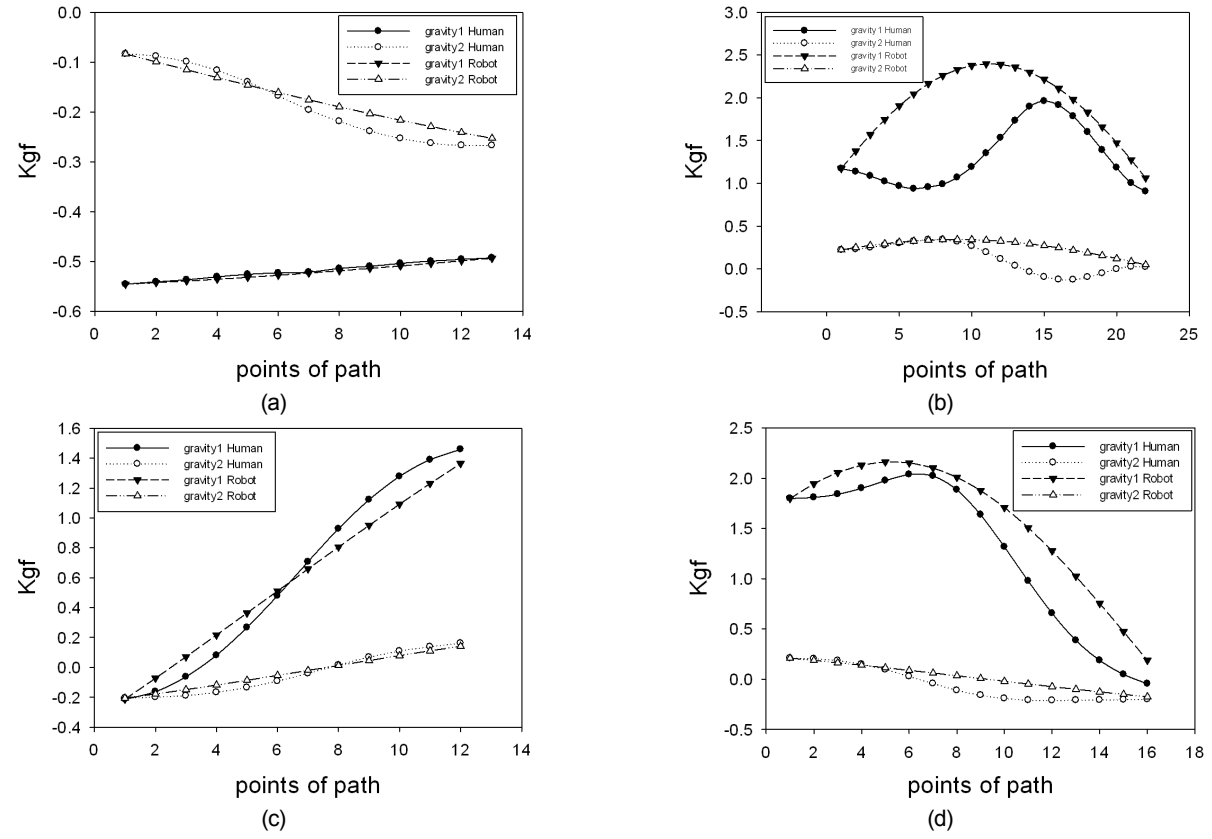

Figure 8. Gravity of human and robot motion patterns of vertical paths (a): Path 3, (b):Path 27 and horizontal paths (c): Path 13, (d): Path 30.

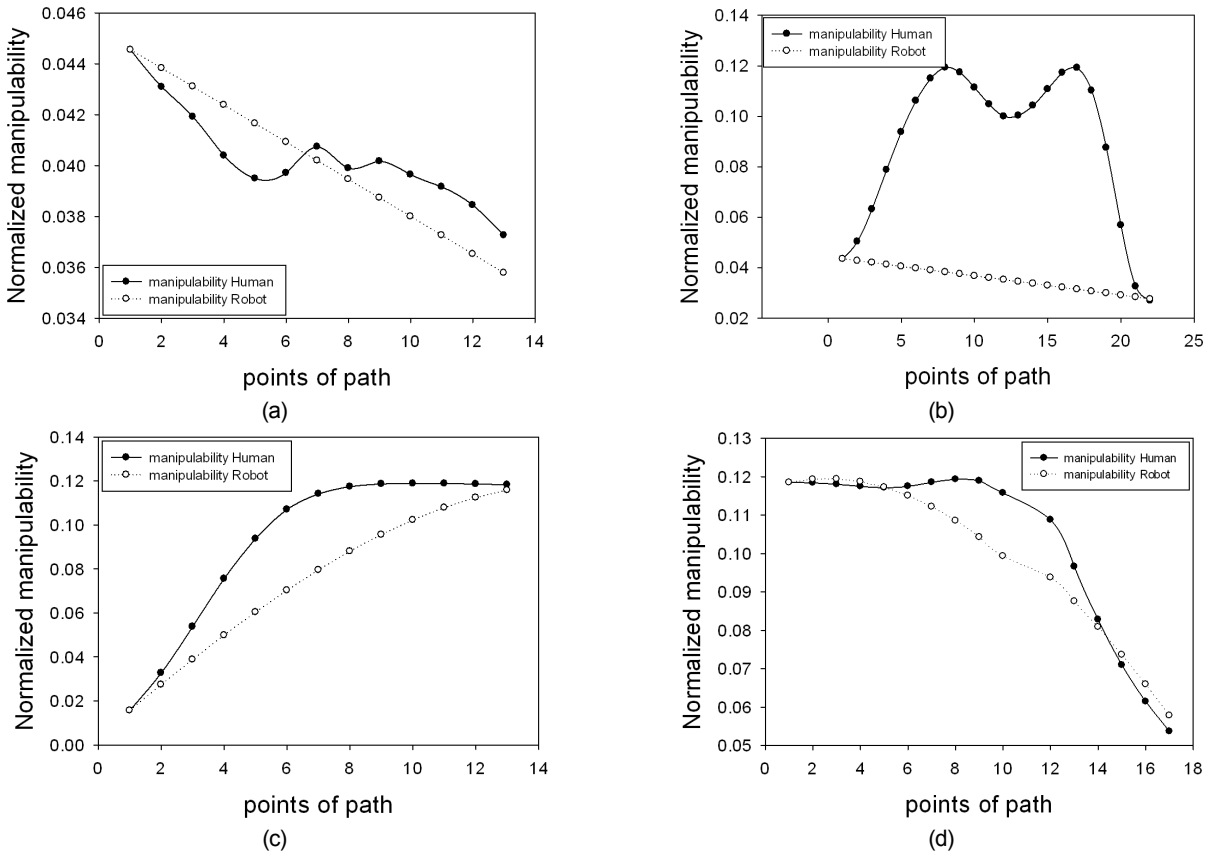

Figure 9. Manipulability measure of human and robot motion patterns of vertical paths (a): Path 3, (b):Path 27 and horizontal paths (c): Path 13, (d): Path 30.

that shows how easily the position and posture can be altered. Thus the fact that manipulability of a human motion pattern is greater than that of a robot motion pattern signifies the task of raising the arm was executed more easily under the human motion pattern. Manipulability increases as the elbow joint bends more but decreases if the angle exceeds 90° as Figure 9(b) shows.

Conclusions

As demands for robots are becoming more diverse, determining the appropriate motion path of a robot especially for pick-and-place tasks in a non-standardized environment is of paramount importance. Humans have become capable of coping with most of predicted or unpredicted handling situations through evolution and learning. Especially in the tasks of pick-and-place whose arm trajectories were not specified exclusively, developing a human like arm motion would be the best alternative for the robot arm to perform a near optimum motion in the viewpoints of the total energy consumption, the required maximum joint torques, the minimum time to achieve the task, and so on.

This research suggested applying the motion of the human arm to the robot arm as an alternative to such pick-and-place unpredictability and analyzed the mechanics and dynamics of 112 motion paths of human and robot arms in order to assess its feasibility. As a result it was observed the human arm tends to move with the elbow bent, which played a pivotal role in improving the manipulability and lowering gravitational force and torque by decreasing distance of moment arm. In addition, energy required for the movement was reduced. This phenomenon was more apparent in vertical rather than horizontal motion, and in long paths rather than short paths. Thus the abrasion of joints could be minimized by reducing load on the bones, muscles, and joints. This signifies efficient use of the motor will be possible in the aspect of energy and durability when the human arm motion is applied to the robot arm motion.

Difference of motion strategy between human arm and

usual industrial robot arm were shown and analyzed dynamically. The existence and amount of the load at the end-effector tend to determine the human arm configuration for the simple pick-and-place motion. The effect of the load at the end such as hand(end-effector) increases dramatically because of the moment effect under the stretched state of the arm in either horizontal or vertical motion. If the scheme of human arm motion can be adopted properly in the motion control of the robot arm, even a light weight robot can perform diverse handling tasks by the maximum utilization of torque capacity of each joint actuator.

As further research, finding out the efficient way of implementing human arm motion as near optimum strategy to the motion controller of an industrial or humanoid robot arm will be strongly suggested.

Conflict of Interest

No potential conflict of interest relevant to this article was reported.

References

Asada, H. and J. J. E. Slotine. 1986. Robot Analysis and Control. John Wiley & Sons, Inc., pp. 93-118.

Asfour, T., K. Berns and R. Dillmann. 2000. The humanoid robot ARMAR: Design and control. In: *The 1st IEEE-RAS International Conference on Humanoid Robots,* pp. 7-8, Boston, USA.

Bae, Y. C., H. Y. Choi and Y. S. Moon. 2007. The Design of Robot Arm based on the Morphological, Neurological Model of Human. Journal of fuzzy logic and intelligent systems 17(4):500-505 (In Korean, with English abstract).

Choi, Y. J. 2007. Study on motion generation of humanoid robot by using motion capture. MS thesis. Suwon, Sungkyunkwan University, Department of Mechanical Engineering

Choi, D. Y. 2006. Intelligent actuation of robot manipulator based on human arm motion behavior. PhD diss. Suwon, Sungkyunkwan University, Department of Bio-Mechatronics.

Jeong, L. W. 2003. Motion Generation of A Humanoid Robot by Using Motion Capture Data. MS thesis. Daejeon, Kaist: Korea Advanced Institute of Science, Department of Electrical Engineering &Computer Science Division of Computer Science.

Kodek, T and M. Munih. 2003. An analysis of static and dynamic joint torques in elbow flexion-extension movements. Simulation Modelling Practice and Theory 11 (3-4):297-311.

Lee, J. W. 2007. Development of Algorithm for Robot Manipulator based on Human Arm motion behavior. MS thesis. Suwon, Sungkyunkwan University, Department of Bio-Mechatronics.

Maurel, W, D. Thalmann, P. Hoffmeyer, P. Beylot, P. Gingins, P. Kalra and N. Magnenat Thalmann. 1996. A biomechanical musculoskeletal model of human upper limb for dynamic simulation. In: Proceedings of the Eurographics workshop on Computer animation and simulation '96, pp.121-136, Poitiers, France.

Potkonjak, V., D. Kostic, S. Tzafestas, M. Popovic, M. Lazarevic and G. Djordjevic. 2001. Human-like behavior of robot arms: general considerations and the handwriting task Part II : the robot arm in handwriting. Robotics and Computer Integrated Manufacturing 17(4):305-315.

Pollard, N., J. K. Hodgins, M. Riley and C. G. Atkeson. 2002. Adapting human motion for the control of a humanoid robot. In: *IEEE International Conference on Robotics and Automation (ICRA 2002)*, pp. 1390-1397.

Sciavicco, L and B. Siciliano. 1988. A solution algorithm to the inverse kinematic problem for redundant manipulators. Robotics and Automation 4(4):403-410.

Yoshikawa, T. 1985. Manipulability of Robotic Mechanisms. The International Journal of Robotics Research 4(2):3-9.